Measurement of the charging state of 4-70 nm aerosols

Enghoff, Martin Andreas Bødker; Svensmark, Jacob

Published in:
Journal of Aerosol Science

Link to article, DOI:
10.1016/j.jaerosci.2017.08.009

Publication date:
2017

Document Version
Peer reviewed version

Measurement of the charging state of 4-70 nm aerosols

Martin Bødker Enghoff[a,*], Jacob Svensmark[a]

[a] *National Space Institute, Danish Technical University, Elektrovej 327, 2800 Kgs. Lyngby, Denmark*

Abstract

The charging state of aerosols in an 8 m^3 reaction chamber was measured using an electrostatic classifier with a condensation particle counter at different levels of ionization in the chamber. By replacing the Kr-85 neutralizer in the classifier with a radioactively neutral dummy we were able to measure only the aerosols that were charged inside our reaction chamber. These measurements were then compared with measurements using the neutralizer to get the charging state of the aerosols, which refers to the charged fraction of the aerosols compared to an equilibrium charge distribution. Charging states were measured for both positively and negatively charged aerosols while the ionization in the chamber was varied using external gamma sources. We find that the negatively charged aerosols were overcharged (relative to the equilibrium) by up to about a factor of 10 below 10 nm and at 16±2% from 10 to 70 nm. At higher levels of radiation on the chamber the smaller aerosols were less overcharged while the large aerosols were more overcharged (23±2%). For the positively charged aerosols only the smallest aerosols were overcharged while those over 10 nm were undercharged (relative to the equilibrium) by 21±3%. Increasing the radiation on the chamber increased the undercharge above 10 nm to 25±2% while the overcharge below 10 nm disappeared. The split between positive and negative charges above 10 nm can be explained by differences in mobility of small negative and positive ions. The overcharge below 10 nm can be explained by ions participating in the formation of aerosols of both signs, while the reduction in this overcharge at higher levels of ionization may be explained by faster recombination.

Keywords: `Aerosols`, Charging state, Experiments, Ion induced nucelation, Reaction chamber

1. Introduction

The atmosphere is constantly being ionized by cosmic rays (Neher, 1971) resulting in ion production rates of typically ~ 2 cm^{-3} s^{-1} at ground level up

*Corresponding author
Email address: `enghoff@space.dtu.dk` (Martin Bødker Enghoff)
URL: `www.space.dtu.dk` (Martin Bødker Enghoff)

to $\sim$ 40 cm^{-3} s^{-1} at about 13 km above ground (Bazilevskaya et al., 2008). Further ionization can happen due to terrestrial sources such as radon and gamma rays (Laakso et al., 2004). The resulting ions interact with atmospheric aerosols, charging them. Supposing that there is time for a charge equilibrium to be established the resulting charge distribution can be calculated (Wiedensohler, 1988).

Ions have long been investigated for their role in cloud formation (Dickinson, 1975; Marsh and Svensmark, 2000), particularly through their effect on aerosol processes (Enghoff and Svensmark, 2008; Kazil et al., 2008). Atmospheric observations at 12 different European sites showed that ions accounted for 1–30% of the nucleation of new aerosols (Manninen et al., 2010). Since ions can stabilize small clusters nucleation by ions is favoured in clean conditions where there is insufficient material for other types of nucleation to be dominant (Kirkby et al., 2011; Pedersen et al., 2012). At higher altitudes with lower temperatures other types of nucleation such as condensation of highly oxygenated molecules also comes into play (Bianchi et al., 2016).

Recently observational evidence from sudden decreases in cosmic radiation due to Solar coronal mass ejections has strengthened the idea of ions influencing clouds through aerosol processes (Svensmark et al., 2016). On the other hand global models predict a very weak effect of ions on cloud formation (Pierce and Adams, 2009; Dunne et al., 2016). One way to assess the influence of ions on aerosol processes is by investigating the charging state of the aerosols. The charging state is defined as the fraction of aerosols with a charge relative to the charged fraction of aerosols in equilibrium with ions (Laakso et al., 2007), where ions are small air ions of sizes below the critical cluster size ($\sim$2 nm) (Kulmala et al., 2007). If the charging state of an aerosol size distribution differs from the equilibrium distribution it can indicate that ions are participating actively in the formation and/or growth of the aerosols (Laakso et al., 2007), however under certain conditions any effect from charging of freshly nucleated aerosols may be lost before the aerosols reach detectable sizes (Kerminen et al., 2007). Previously measurements of the charging state of aerosols have been used to characterize growth rates and the contributions from ions to aerosol formation in atmospheric observations (Leppa et al., 2013; Vana et al., 2006) and also in soot formation (Maricq, 2004).

In this work we want to investigate the size distribution of the charging state of sulphuric acid-water aerosols in an experimental setup that has previously shown a significant effect of ions on nucleation (Svensmark et al., 2007; Svensmark et al., 2013) to learn more about exactly how the ions influence the generated aerosols. We do this by measuring the positive and negative charging state of the aerosols while varying the ionization level.

2. Materials and methods

The aerosols were generated in an 8 m^3 stainless steel reaction chamber which has been previously described (Svensmark et al., 2013) - see Fig. 1 for

the current setup. The method of aerosol generation was nucleation of sulphuric acid aerosols, started by photolysis of ozone using UV lamps (253.7 nm), resulting in hydroxyl radicals that oxidise SO_2 into sulphuric acid. The resulting aerosol concentration was between 1000-5000 cm^{-3}. While only water and sulphuric acid were added intentionally we cannot rule out a contribution to the nucleation of aerosols from e.g. ammonia, which was not measured. The ionization in the chamber could be controlled using two 27 MBq Cs-137 gamma sources with varying amounts of lead in front, giving ion production rates (q) of about 16-200 cm^{-3} s^{-1}. The size distribution of the aerosols was measured by a Scanning Mobility Particle Sizer (SMPS) system consisting of a TSI model 3080 electrostatic classifier, with a model 3085 nano Differential Mobility Analyzer (DMA) which has an adjustable size range of 2-150 nm (set to 2-70 nm in this study) and model 3775 Condensation Particle Counter (CPC). We note that the counting efficiency of the CPC decreases for sizes below 10-15 nm and that the CPC has a 50% cut-off at about 5 nm depending on material (4.2 nm for silver particles and 6.7 nm for NaCl) (Hermann et al., 2007) and that the cut-off for sulphuric acid aerosols is not known exactly. Also note that all aerosol sizes mentioned refer to the mobility diameter (Hinds, 1999), taking advantage of the relation between electrical mobility and particle size, since geometric diameter is not something which is well defined for small sizes. The system was attached directly to the reaction chamber with a 45 cm sampling line protuding into the chamber and with an additional 140 cm between the chamber and the SMPS inlet (the 140 cm were reduced to 30 cm for some experiments to test the influence of the length of the sampling tube). The instrument was operated with a sheath flow of 15 L min^{-1}, a bypass flow of 5 L min^{-1}, and a flow to the CPC of 1.5 L min^{-1}. The classifier was equipped with a TSI model 3077A Kr-85 aerosol neutralizer.

The objective is to measure the actual charging state of the aerosols before they enter the classifier. Since the Kr-85 neutralizer gives the aerosols an equilibrium charge distribution these measurements cannot be used alone to infer the charging state. By removing the Kr-85 neutralizer we can measure the aerosols that are actually charged in the reaction chamber. However simply removing the neutralizer or replacing it with tubing changes the flow pattern in the instrument so we installed a dummy neutralizer, made exactly like the 3077A but without any Kr-85. By making sequential measurements where the Kr-85 neutralizer was replaced with the dummy and dividing the resulting aerosol distributions with each other we find the charging state, which is the actual charge distribution of the aerosols relative to the equilibrium distribution obtained in the SMPS system. This relative technique also reduces the impact of the length of the sampling tube and other instrument artifacts, which can have implications for normal size distribution measurements due to size dependent losses. The technique is similar in concept to the Ion-DMPS that was previously used in the laboratory and on field campaigns(Laakso et al., 2007). A similar method has also been applied to investigate the charging state of soot particles (Maricq, 2004). For larger aerosols multiple charging becomes a problem (Järvinen et al., 2017), but in these experiments the issue is negligible (the fraction of aerosols

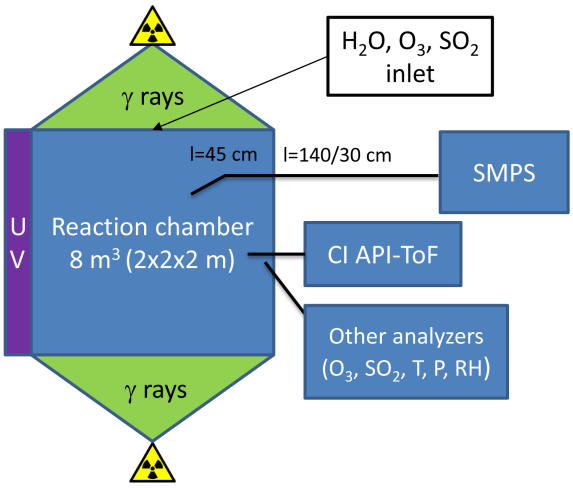

Figure 1: Experimental setup, showing the chamber (top view) with the SMPS-system and its sampling tube, where the length on the outside of the chamber was varied. Also shown are the two Cs-137 gamma sources (one on each side of the chamber) and the UV lamps at the back, as well as a representation of the other analyzers and inlet system (see text and Svensmark et al. (2013) for details).

with 2 charges at 65 nm is ∼1.4% (Wiedensohler, 1988)).

In the standard setup the classifier is equipped with a negative power supply that, due to the construction of the DMA, results in positive aerosols being measured. In order to instead measure negative aerosols the power supply could be replaced with a positive supply, measuring negative aerosols. Both power supplies are the standard models delivered by TSI (Ultravolt 10A12-N4-M and 10A12-P4-M for negative and positive voltages, respectively).

During the experiments the chamber was kept in a steady state where aerosols were continuously being generated and lost to the walls and dilution. After this steady state was achieved the Kr-85 neutralizer and dummy were then interchanged with 2 hour intervals and as such each size distribution was measured for a bit below 2 hours, corresponding to the mean of ∼50 individually measured size distributions (the scan time for the SMPS was 135 seconds). An experiment thus consisted of ∼2 hours of measurement with the Kr-85 neutralizer and ∼2 hours with the dummy, except in one case. The first few scans after each change of the neutralizer were not used since they were disturbed by the process of replacing the neutralizer. Fig. 2 (left side) shows the measured aerosol concentration for two experiments as well as the hours preceding and following the experiments. The right side of Fig. 2 shows the resulting size distributions with and without the neutralizer for one of the experiments, obtained by averaging all scans.

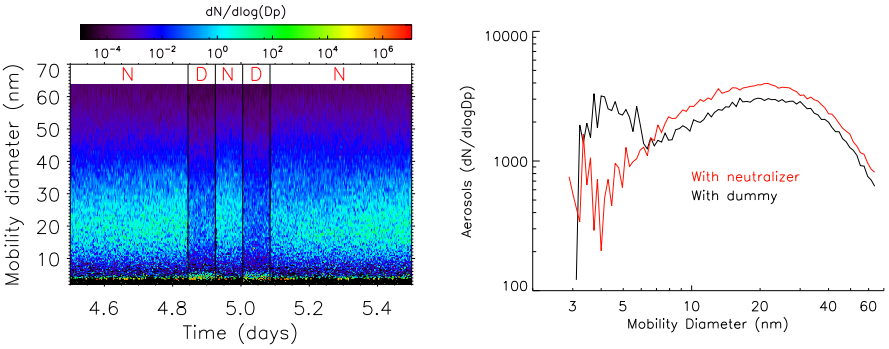

Figure 2: An example of how experiments are made. The left figure shows the evolution of the aerosol size distribution (positively charged aerosols) during two experiments without gamma sources on the chamber. The regions beneath the red "N" and "D" signs correspond to measurements with the neutralizer (N) and with the dummy (D) repectively (see text). The right figure shows the resulting size distributions with and without the Kr-85 charger from the first of the experiments shown on the left.

2.1. Systematic differences between negative and positive measurements

One concern with comparing measurements of positive and negative aerosols is that they may behave slightly different in the SMPS system. This should not be a major concern with these experiments since all the measurements are relative but the sequence of measurements allows a test for this issue nevertheless. We compared two experiments made just before and after the power supply in the SMPS was changed from negative to positive. Both experiments were made with maximum gamma ionization and with the Kr-85 neutralizer. If the positive and negative aerosols behave similarly the two experiments should give the same size distributions. Fig. 3 shows the two size distributions relative to each other with the distribution of the negatively charged aerosols being divided by the positive aerosols. Both size distributions are based on ∼2 hours of measurements as for the other experiments. For sizes above 10 nm the difference between the two size distributions is less than 10%. Below 10 nm the difference increases up to a factor of 2 for the smallest sizes implying that the instrument detects small positive aerosols more effectively. This may make the data below 10 nm more unreliable, although this effect should be reduced since the measurements are relative. One possible reason for the difference in behavior could be if the neutralizer is not efficient enough to achieve the equilibrium distribution such that the initial charging state of the aerosol distribution affects the measurements. It has previously been shown that if the total aerosol concentration is higher than 1/10 of the ion concentration then the charging state does not reach equilibrium (de La Verpilliere et al., 2015), however that is far from the case in this study. Another possible reason could be a voltage offset in the DMA due to using two different power supplies.

2.2. Uncertainties

For each experiment the standard deviation was found. First the standard error of the mean was found for each size bin, utilizing all ∼50 individually measured size distributions for each experiment, with and without the Kr-85 neutralizer. For the relative size distributions the standard deviation was then found through the standard formula for the propagation of random errors. This method was also used to combine the standard deviations for experiments of the same type. All uncertainties are given as 1 standard deviation.

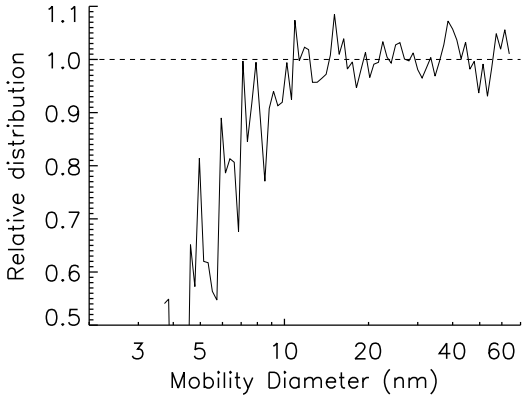

Figure 3: Comparison of experiments done just before and after changing the power supply in the SMPS. The size distribution of negatively charged aerosols was divided by the positively charged aerosols.

3. Results

A total of 21 experiments were done. 6 experiments were done with the negative power supply measuring positive aerosols, consisting of 2 experiments with background ionization on the chamber and 4 with maximum gamma ionization on the chamber, 2 of which were done with the short sampling tube. The main part of the experiments was done with the positive power supply measuring negative aerosols since they are the ions of primary interest for ion induced nucleation (Enghoff and Svensmark, 2008; Kurtén et al., 2009). 15 experiments were done on negative aerosols: 6 with background ionization (2 of these with the short sampling tube), 6 with maximum ionization (2 of these with the short sampling tube), and 3 with 1 cm of lead in front of the gamma source resulting in a reduction in ion production from the gamma sources by 70% and thus the ion concentration was reduced to ∼55%. The experiments are summarized in Table 1 and discussed in detail in the following sections.

Table 1: Overview of the performed experiments, for all combinations of sample line length, sign of aerosols probed, and ion density in the chamber volume. N indicates the number of times the experiment was repeated for a given choice of parameters. The fifth column indicates the average charging state for large aerosols and the final column the average charging state for the smallest aerosols (note that the values are very size dependent and thus the uncertainty is not given - see Fig. 4 for details).

N	Ion charge	Chamber Ionization	Sample line	Overcharge $10\,\mathrm{nm} < D < 70\,\mathrm{nm}$	Overcharge $D < 10\,\mathrm{nm}$
2	+	Background	Long	0.79 ± 0.025	3.06
2	+	Maximum γ	Long	0.75 ± 0.024	0.77
2	+	Maximum γ	Short	0.72 ± 0.023	0.97
4	−	Background	Long	1.16 ± 0.022	2.90
2	−	Background	Short	1.15 ± 0.030	2.50
3	−	1 cm lead	Long	1.22 ± 0.025	2.27
4	−	Maximum γ	Long	1.23 ± 0.021	1.84
2	−	Maximum γ	Short	1.29 ± 0.029	1.73

3.1. Positive aerosols

Figure 4 (left panel) shows the charging state for all experiments with positive aerosols. The charging state is the measurement done with the dummy divided by the measurement done with the Kr-85 neutralizer, which gives the actual charge distribution relative to the equilibrium charge distribution. The average overcharge for diameters above 10 nm without gammas on the chamber was 0.79±0.025. With full exposure to the gamma sources the overcharge was 0.75±0.024 (for one of these experiments there was no measurement with the Kr-85 neutralizer so the two experiments for positively charged aerosols with full gamma exposure use the same measurement with the neutralizer as reference which should be ok since it was done between the two measurements without the neutralizer). Using the shorter sampling tube and full exposure to the gammas the overcharge was 0.72±0.023. Below 10 nm the positive aerosols were overcharged up to about a factor of 10 for the smallest aerosols without exposure to the gamma sources - this effect disappeared with full exposure to the gamma sources.

3.2. Negative aerosols

The results for negative aerosols are shown in Fig. 4, in the right panel. The average overcharge at diameters above 10 nm was 1.16±0.022 when there were no gamma rays on the chamber and 1.23±0.021 with full gamma exposure. When the sampling line was reduced the overcharge was 1.15±0.030 without gammas and 1.29±0.029 with gammas. Using 1 cm of lead in front of the Cs-137 sources, which should reduce the resulting ion concentration to ∼55%, the overcharge above 10 nm was 1.22±0.025 (using the long sampling tube). Below 10 nm the negative aerosols were overcharged slightly more than the positive. In contrast to the positively charged aerosols this effect did not disappear entirely, but did decrease as the ionization was increased.

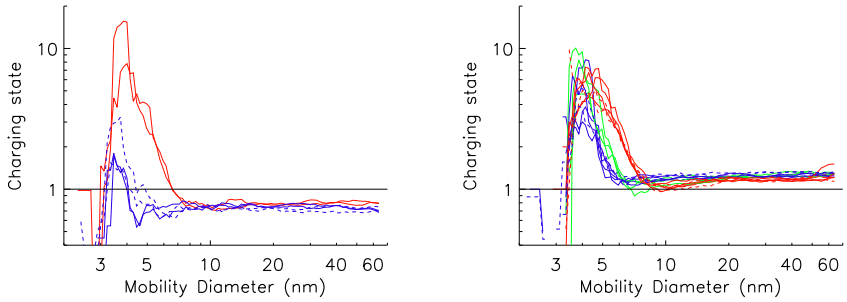

Figure 4: Charging state of positive (left) and negative (right) aerosols, using a 4-point moving average. Blue lines are when the chamber was irradiated by the Cs-137 sources, red lines for when it was not. Green lines are with 1 cm lead in front of the Cs-137 sources. The coloured dashed lines are when the shorter sampling line was used. The black dashed line is simply 1, corresponding to the equilibrium charge distribution. The two fully drawn blue lines in the left figure correspond to the experiments shown in Fig. 2.

4. Discussion and Conclusion

The charging state of laboratory generated positive and negative aerosols was measured. Negatively charged aerosols were found to be overcharged relative to the equilibrium charge distribution at all sizes with an increase in overcharge above 10 nm when the ionization was increased and a corresponding decrease below 10 nm. The positive aerosols were overcharged below 10 nm and undercharged above 10 nm. The splitting between positive and negative charges for aerosols larger than 10 nm seems to increase with increasing ionization. Reducing the length of the sampling tube increased the splitting of charge above 10 nm slightly. Overcharging of small aerosols have previously been reported from atmospheric observations as an indication of nucleation by ion processes (Leppa et al., 2013; Vana et al., 2006; Laakso et al., 2007). The effect of ionization level on charging state was treated theoretically by Kerminen et al. (2007). The differences between negatively and positively charged aerosols stand in contrast to measurements of the charging state of soot aerosols where aerosols of both polarities were equally charged when measuring at least 20 mm from the flame (although there were more negatively charged aerosols at shorter distances) (Maricq, 2004) and to atmospheric observations by Laakso et al. (2007) where aerosols above 10 nm were reported to be close to charge equilibrium even during events where the smaller aerosols were overcharged.

4.1. Above 10 nm

This splitting of charge may simply arise from a difference in electric mobility of the positive and negative small ions. Measurements have shown that natural ions of opposite charges can have different mobilities (Hõrrak et al., 1998), with negative ions being more mobile due to their smaller size (in average). This

difference can affect the charging state of aerosols since the collision frequencies between ions and aerosols will be different for positive and negative ions. Note that the SMPS system already assumes a slight difference in charging on positive and negative aerosols with a ratio of ion mobilities Z_+/Z_- of 0.875 (Wiedensohler, 1988).

A simple model based on the following equations can be used to calculate the expected split of positive and negative charges:

$$\frac{dn^+}{dt} = q - \alpha n^+ n^- - n^+ \beta^{+0} N^0 - n^+ \beta^{+-} N^- \quad (1)$$

$$\frac{dn^-}{dt} = q - \alpha n^+ n^- - n^- \beta^{-0} N^0 - n^- \beta^{-+} N^+ \quad (2)$$

$$\frac{dN^0}{dt} = n^+ \beta^{+-} N^- + n^- \beta^{-+} N^+ - n^+ \beta^{+0} N^0 - n^- \beta^{-0} N^0 \quad (3)$$

$$\frac{dN^+}{dt} = n^+ \beta^{+0} N^0 - n^- \beta^{-+} N^+ \quad (4)$$

$$\frac{dN^-}{dt} = n^- \beta^{-0} N^0 - n^+ \beta^{+-} N^- \quad (5)$$

where q is the ion production rate, n^+ is small positive ions, n^- is small negative ions, N^0 is neutral aerosols, N^+ is positive aerosols, N^- is negative aerosols, α is the ion-ion recombination coefficient, and betas are the interaction coefficients between aerosols and ions (Hoppel and Frick, 1986). It is assumed that there is no interaction (coagulation) between aerosols which is reasonable for aerosol concentrations of a few thousand cm^{-3}. The interaction coefficients used assume a mass of 150/90 amu for positive/negative ions - using an empirical relation between mass and mobility (Tammet, 1995) the mobility ratio for 152/90 amu is 0.798 which is a slightly larger difference than used in the SMPS system, which should cause a larger split between positive and negative aerosols.

Figure 5 shows the difference in charged fraction for different aerosol sizes, as a function of the ion production rate (q), where the above equations have been solved independently for 3 different aerosol sizes and 30 values of q. This demonstrates that a split in charge can occur simply due to a difference in mobility and that the split can increase when the ion production rate is increased. Thus the experimental results where the difference in charging between positive and negative aerosols increase with increasing ionization above 10 nm can be explained in this way, although it is not possible to make a quantitative estimate due to lack of information on the actual ion masses in the experiments.

4.2. Below 10 nm

The high overcharge below 10 nm and the following reduction in this overcharge when the ionization is increased cannot be explained by the model presented in the previous section and another mechanism may be at work. Previously it has been shown that an overcharge in small aerosols may indicate

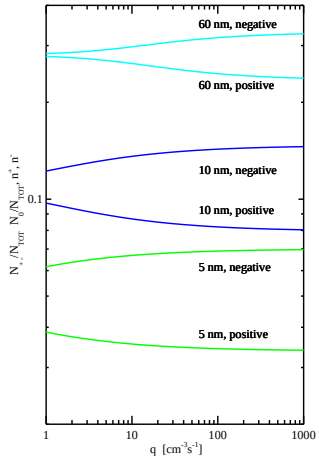

Figure 5: Charge distributions of aerosols as a function of ionization level, found by solving Equations 1-5 for 30 values of the ion production rate (q). Each colour corresponds to a given size with the top branch showing negatively charged aerosols and the bottom branch positively charged aerosols. The total number of aerosol particles is $N_{tot} = N^0 + N^- + N^+ = 3000\,\mathrm{cm}^{-3}$.

that the ions have been active in the nucleation of the aerosols (Leppa et al., 2013). Laakso et al. (2007) found that both negative and positive aerosols could be overcharged during nucleation events, but with a preference for negatively charged aerosols, like in the present measurements. If the aerosols nucleate with a charge and thus are heavily overcharged from the beginning then the observation that the overcharge for both positive and negative aerosols below 10 nm goes down (and totally disappears in the case of positive aerosols) when the ion production is increased could be due to faster recombination times. To test this we use the charging theory previously described by Kerminen et al. (2007, eq. 15) and Laakso et al. (2007, eq. 1) where the charging state relative to the equilibrium state ($S(d_p)$) is found:

$$S(d_p) = 1 - \frac{1}{Kd_p} + \frac{1 + (S_0 - 1)Kd_0}{Kd_p} e^{-K(d_p - d_0)} \tag{6}$$

where S_0 is the charging state at a reference diameter (d_0 - in this case 1.7 nm) and K is a parameter given as

$$K = \frac{\alpha n_{\pm}}{GR(d_p)} \tag{7}$$

where $n_{\pm}$ is the small ion concentration (assumed equal for both signs), α is the ion-ion recombination coefficient, and GR is the growth rate of the aerosols. $n_{\pm}$ is set to $(q\alpha)^{0.5}$ (based on a steady state assumption) and the ion

production rate (q) is 16 cm^{-3} s^{-1} without gamma ionization and 200 cm^{-3} s^{-1} with full power on the gamma sources, based on a set of measurements of the ion current with a Gerdien tube (Gerdien, 1905) performed previous to the experiments. The growth rate (GR) is set to $\frac{[SA]}{10^7 cm^{-3} nm^{-1} s}$ where the sulphuric acid concentration [SA] is $1.7 \cdot 10^8$ cm^{-3} found as an average of 6 days of measurements performed during part of the experiments using a CI-API-ToF mass spectrometer (Jokinen et al., 2012). Due to uncertainties in the calibration of the CI-API-ToF the sulphuric acid concentration is estimated to have an uncertainty of a factor of 2.

Fig. 6 shows the results for the positive (left panel) and negative aerosols (right panel). The measured overcharge with and without gamma sources for sizes below 10 nm is shown along with theoretical curves using Eq. 6. The initial overcharge (S_0) has been set using the assumption that all aerosols are formed with a charge at 1.7 nm, which is probably optimistic (the critical cluster size is not known for the system, we choose 1.7 nm since it is the size nucleation rates are commonly reported at (e.g. Dunne et al. (2016)). It is seen that the decrease in overcharge when the gamma ionization is increased is explained qualitatively by the theory - when the ionization goes up the aerosols which are nucleated with a charge are neutralized faster. As the sizes approach 10 nm all information on the initial charging state is lost and the charge splitting due to mobility differences of negative and positive ions starts to dominate the charging state. Since there are rather large uncertainties in both [SA], S_0, and to some degree q an accurate estimation of the magnitude of the decrease in overcharge is not realistically possible. In the data it seems that the overcharge drops for sizes below 4 nm, but we note that this is close to the 50%cut-off of the CPC so for these sizes the measurements are less reliable. That the overcharge on the negative aerosols is larger than on the positive can be explained either by a preference for negative nucleation due to different chemical composition of the negatively and positively charged aerosols or due to mobility differences between positive and negative small ions - the positive aerosols are neutralized by smaller more mobile negative ions while the negative ions are neutralized by larger positive ions and therefore retain their overcharge slightly longer.

The results for sizes below 10 nm do support that the aerosols are nucleated with a charge and that both positive and negative aerosols are nucleated.

5. Acknowledgements

The authors thank Henrik Svensmark for insightful discussions on the interpretation of the data and Bent Hansen of Danalytic for his assistance with preparing the SMPS system for the measurements. This research did not receive any specific grant from funding agencies in the public, commercial, or not-for-profit sectors.

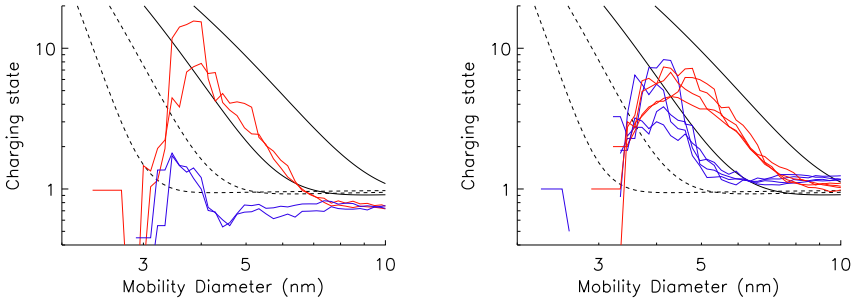

Figure 6: Charging state of positive aerosols (left) and negative aerosols (right) for sizes below 10 nm. The curves have been smoothed with a 4 point running mean. Red curves are experiments without gamma ionization on the chamber, blue curves are with gammas on the chamber. The fully drawn back lines are the theoretical curves (see text) for an ion production rate of 16 cm^{-3} s^{-1} where the growth rate is varied by a factor of 2. The dashed black lines are the same but for an ion production rate of 200 cm^{-3} s^{-1}.

References

Bazilevskaya, G.A., Usoskin, I.G., Flückiger, E.O., Harrison, R.G., Desorgher, L., Bütikofer, R., Krainev, M.B., Makhmutov, V.S., Stozhkov, Y.I., Svirzhevskaya, A.K., Svirzhevsky, N.S., Kovaltsov, G.A., 2008. Cosmic Ray Induced Ion Production in the Atmosphere. Space Science Reviews 137, 149–173. doi:10.1007/s11214-008-9339-y.

Bianchi, F., Trostl, J., Junninen, H., Frege, C., Henne, S., Hoyle, C.R., Molteni, U., Herrmann, E., Adamov, A., Bukowiecki, N., Chen, X., Duplissy, J., Gysel, M., Hutterli, M., Kangasluoma, J., Kontkanen, J., Kuerten, A., Manninen, H.E., Muench, S., Perakyla, O., Petaja, T., Rondo, L., Williamson, C., Weingartner, E., Curtius, J., Worsnop, D.R., Kulmala, M., Dommen, J., Baltensperger, U., 2016. New particle formation in the free troposphere: A question of chemistry and timing. SCIENCE 352, 1109–1112. doi:{10.1126/science.aad5456}.

Dickinson, R.E., 1975. Solar variability and the lower atmosphere. Bulletin American Meteorological Society 56, 1240–1248.

Dunne, E.M., Gordon, H., Kürten, A., Almeida, J., Duplissy, J., Williamson, C., Ortega, I.K., Pringle, K.J., Adamov, A., Baltensperger, U., Barmet, P., Benduhn, F., Bianchi, F., Breitenlechner, M., Clarke, A., Curtius, J., Dommen, J., Donahue, N.M., Ehrhart, S., Flagan, R.C., Franchin, A., Guida, R., Hakala, J., Hansel, A., Heinritzi, M., Jokinen, T., Kangasluoma, J., Kirkby, J., Kulmala, M., Kupc, A., Lawler, M.J., Lehtipalo, K., Makhmutov, V., Mann, G., Mathot, S., Merikanto, J., Miettinen, P., Nenes, A., Onnela, A., Rap, A., Reddington, C.L.S., Riccobono, F., Richards, N.A.D., Rissanen,

M.P., Rondo, L., Sarnela, N., Schobesberger, S., Sengupta, K., Simon, M., Sipilä, M., Smith, J.N., Stozkhov, Y., Tomé, A., Tröstl, J., Wagner, P.E., Wimmer, D., Winkler, P.M., Worsnop, D.R., Carslaw, K.S., 2016. Global atmospheric particle formation from cern cloud measurements. Science 354. doi:10.1126/science.aaf2649.

Enghoff, M.B., Svensmark, H., 2008. The role of atmospheric ions in aerosol nucleation - a review. Atmospheric Chemistry and Physics 8, 4911–4323. doi:10.5194/acp-8-4911-2008.

Gerdien, H., 1905. Demonstration eines apparates zur absoluten messung der elektrischen leitfahigheit der luft. Phys. Zeitung 6, 800–801.

Hermann, M., Wehner, B., Bischof, O., Han, H.S., Krinke, T., Liu, W., Zerrath, A., Wiedensohler, A., 2007. Particle counting efficiencies of new tsi condensation particle counters. Journal of Aerosol Science 38, 674–.682. doi:doi:10.1016/j.jaerosci.2007.05.001.

Hinds, W.C., 1999. Aerosol Technology. John Wiley and Sons.

Hoppel, W.A., Frick, G.M., 1986. Ion-aerosol attachment coefficients and the steady-state charge distribution on aerosols in a bipolar ion environment. Aerosol Science and Technology 5, 1–21. doi:10.1080/02786828608959073.

Hõrrak, U., Salm, J., Tammet, H., 1998. Bursts of intermediate ions in atmospheric air. Journal of Geophysical Research 103, 13909–13915. doi:10.1029/97JD01570.

Järvinen, A., Heikkilä, P., Keskinen, J., Yli-Ojanperä, J., 2017. Particle charge-size distribution measurement using a differential mobility analyzer and an electrical low pressure impactor. Aerosol Science and Technology 51, 20–29. doi:10.1080/02786826.2016.1256469.

Jokinen, T., Sipilä, M., Junninen, H., Ehn, M., Lönn, G., Hakala, J., Petäjä, T., Mauldin III, R.L., Kulmala, M., Worsnop, D.R., 2012. Atmospheric sulphuric acid and neutral cluster measurements using ci-api-tof. Atmospheric Chemistry and Physics 12, 4117–4125. URL: http://www.atmos-chem-phys.net/12/4117/2012/, doi:10.5194/acp-12-4117-2012.

Kazil, J., Harrison, R.G., Lovejoy, E.R., 2008. Tropospheric new particle formation and the role ofions. Space Science Reviews 137, 241–255. URL: http://dx.doi.org/10.1007/s11214-008-9388-2, doi:10.1007/s11214-008-9388-2.

Kerminen, V.M., Anttila, T., Petäjä, T., Laakso, L., Gagné, S., Lehtinen, K.E.J., Kulmala, M., 2007. Charging state of the atmospheric nucleation mode: Implications for separating neutral and ion-induced nucleation. Journal of Geophysical Research (Atmospheres) 112, 21205–+. doi:10.1029/2007JD008649.

Kirkby, J., Curtius, J., Almeida, J., Dunne, E., Duplissy, J., Ehrhart, S., Franchin, A., Gagné, S., Ickes, L., Kürten, A., Kupc, A., Metzger, A., Riccobono, F., Rondo, L., Schobesberger, S., Tsagkogeorgas, G., Wimmer, D., Amorim, A., Bianchi, F., Breitenlechner, M., David, A., Dommen, J., Downard, A., Ehn, M., Flagan, R.C., Haider, S., Hansel, A., Hauser, D., Jud, W., Junninen, H., Kreissl, F., Kvashin, A., Laaksonen, A., Lehtipalo, K., Lima, J., Lovejoy, E.R., Makhmutov, V., Mathot, S., Mikkilä, J., Minginette, P., Mogo, S., Nieminen, T., Onnela, A., Pereira, P., Petäjä, T., Schnitzhofer, R., Seinfeld, J.H., Sipilä, M., Stozhkov, Y., Stratmann, F., Tomé, A., Vanhanen, J., Viisanen, Y., Vrtala, A., Wagner, P.E., Walther, H., Weingartner, E., Wex, H., Winkler, P.M., Carslaw, K.S., Worsnop, D.R., Baltensperger, U., Kulmala, M., 2011. Role of sulphuric acid, ammonia and galactic cosmic rays in atmospheric aerosol nucleation. Nature 476, 429–433. doi:10.1038/nature10343.

Kulmala, M., Riipinen, I., Sipilä, M., Manninen, H.E., Petäjä, T., Junninen, H., Maso, M.D., Mordas, G., Mirme, A., Vana, M., Hirsikko, A., Laakso, L., Harrison, R.M., Hanson, I., Leung, C., Lehtinen, K.E.J., Keminen, V.M., 2007. Towards direct measurement of atmospheric nucleation. Science 318, 89–92.

Kurtén, T., Ortega, K.I., Vehkamäki, H., 2009. The sign preference in sulfuric acid nucleation. Journal of Molecular Structure: THEOCHEM 901, 169–173. doi:10.1016/j.theochem.2009.01.024.

de La Verpilliere, J.L., Swanson, J.J., Boies, A.M., 2015. Unsteady bipolor diffusion charging in aerosol neutralisers: A non-dimension approach to predict charge distribution equilibrium behaviour. Journal of Aerosol Science 86, 55–68. doi:10.1016/j.jaerosci.2015.03.006.

Laakso, L., Anttila, T., Lehtinen, K.E.J., Aalto, P.P., Kulmala, M., Hõrrak, U., Paatero, J., Hanke, M., Arnold, F., 2004. Kinetic nucleation of ions in boreal forest particle formation events. Atmospheric Chemistry and Physics 4, 2353–2366.

Laakso, L., Gagné, S., Petäjä, T., Hirsikko, A., Aalto, P.P., Kulmala, M., Kerminen, V.M., 2007. Detecting charging state of ultra-fine particles: instrumental development and ambient measurements. Atmospheric Chemistry and Physics 7, 1333–1345.

Leppa, J., Gagne, S., Laakso, L., Manninen, H.E., Lehtinen, K.E.J., Kulmala, M., Kerminen, V.M., 2013. Using measurements of the aerosol charging state in determination of the particle growth rate and the proportion of ion-induced nucleation. ATMOSPHERIC CHEMISTRY AND PHYSICS 13, 463–486. doi:{10.5194/acp-13-463-2013}.

Manninen, H.E., Nieminen, T., Asmi, E., Gagne, S., Hakkinen, S., Lehtipalo, K., Aalto, P., Vana, M., Mirme, A., Mirme, S., Horrak, U., Plass-Duelmer,

C., Stange, G., Kiss, G., Hoffer, A., Toeroe, N., Moerman, M., Henzing, B., de Leeuw, G., Brinkenberg, M., Kouvarakis, G.N., Bougiatioti, A., Mihalopoulos, N., O'Dowd, C., Ceburnis, D., Arneth, A., Svenningsson, B., Swietlicki, E., Tarozzi, L., Decesari, S., Facchini, M.C., Birmili, W., Sonntag, A., Wiedensohler, A., Boulon, J., Sellegri, K., Laj, P., Gysel, M., Bukowiecki, N., Weingartner, E., Wehrle, G., Laaksonen, A., Hamed, A., Joutsensaari, J., Petaja, T., Kerminen, V.M., Kulmala, M., 2010. EUCAARI ion spectrometer measurements at 12 European sites - analysis of new particle formation events. ATMOSPHERIC CHEMISTRY AND PHYSICS 10, 7907–7927. doi:{10.5194/acp-10-7907-2010}.

Maricq, M.M., 2004. Size and charge of soot particles in rich premixed ethylene flames. Combustion and Flame 137, 340–350. doi:10.1016/j.combustflame.2004.01.013.

Marsh, N.D., Svensmark, H., 2000. Low Cloud Properties Influenced by Cosmic Rays. Physical Review Letters 85, 5004–5007. doi:10.1103/PhysRevLett.85.5004, arXiv:arXiv:physics/0005072.

Neher, H.V., 1971. Cosmic rays at high latitudes and altitudes covering four solar maxima. Journal of Geophysical Research 79, 1637–1651.

Pedersen, J.O.P., Enghoff, M.B., Paling, S.M., Svensmark, H., 2012. Aerosol nucleation in an ultra-low ion density environment. JOURNAL OF AEROSOL SCIENCE 50, 75–85. doi:{10.1016/j.jaerosci.2012.03.003}.

Pierce, J.R., Adams, P.J., 2009. Can cosmic rays affect cloud condensation nuclei by altering new particle formation rates? Geophysical Research Letters 36, 9820. doi:10.1029/2009GL037946.

Svensmark, H., Enghoff, M.B., Pedersen, J.O.P., 2013. Response of cloud condensation nuclei (> 50 nm) to changes in ion-nucleation. Physics Letters A 377, 2343–2347. doi:10.1016/j.physleta.2013.07.004.

Svensmark, H., Pedersen, J.O.P., Marsh, N.D., Enghoff, M.B., Uggerhøj, U.I., 2007. Experimental evidence for the role of ions in particle nucleation under atmospheric conditions. Proceedings of the Royal Society A 463, 385–396.

Svensmark, J., Enghoff, M.B., Shaviv, N.J., Svensmark, H., 2016. The response of clouds and aerosols to cosmic ray decreases. Journal of Geophysical Research: Space Physics , 8152–8181doi:10.1002/2016JA022689. 2016JA022689.

Tammet, H., 1995. Size and mobility of nanometer particles, clusters and ions. Journal of Aerosol Science 26, 459–476.

Vana, M., Tamm, E., Hõrrak, U., Mirme, A., Tammet, H., Laakso, L., Aalto, P.P., Kulmala, M., 2006. Charging state of atmospheric nanoparticles during the nucleation burst events. Atmospheric Research 82, 536–546.

Wiedensohler, A., 1988. An approximation of the bipolar charge distribution for particles in the submicron size range. Journal of Aerosol Science 19, 387–389. doi:http://dx.doi.org/10.1016/0021-8502(88)90278-9.